Acta Cryst. (1981). B37, 591–597

Studies of Monoclinic Hen Egg White Lysozyme. I. Structure Solution at 4 Å Resolution and Molecular-Packing Comparisons with Tetragonal and Triclinic Lysozymes

BY J. HOGLE,* S. T. RAO, M. MALLIKARJUNAN,† C. BEDDELL,‡ R. K. MCMULLAN§ AND M. SUNDARALINGAM‖

Department of Biochemistry, College of Agricultural and Life Sciences, University of Wisconsin–Madison, Madison, Wisconsin 53706, *USA*

(*Received* 22 *May* 1980; *accepted* 27 *October* 1980)

Abstract

Monoclinic crystals of hen egg white lysozyme have been grown in two morphologically indistinguishable forms (*M*1 and *M*2); both have the same space group $P2_1$ with two independent molecules in the asymmetric unit and very similar cell constants (*M*1: $a = 28{\cdot}0$, $b = 62{\cdot}9$, $c = 60{\cdot}5$ Å, $\beta = 90{\cdot}8°$; *M*2: $a = 27{\cdot}5$, $b = 63{\cdot}5$, $c = 60{\cdot}3$ Å, $\beta = 90{\cdot}5°$). *M*1 can be readily grown at low pH (below 6·8) while *M*2 can be grown at higher pH (above 7). The structure of the *M*1 form has been solved from a 4 Å MIR map phased with four heavy-atom derivatives [PCMBS I, PCMBS II, $Hg(NO_3)_2$ and $UO_2(NO_3)_2$] and the backbone chain traced. The transformations relating the tetragonal structure to the monoclinic structure have been obtained. The two independent molecules are related by a pseudo 2_1 axis which runs nearly parallel to and midway between the crystallographic 2_1 axis. The molecules are tightly packed and their active-site clefts are partially blocked by the *C*-terminal region of the screw-axis-related molecule. The heavy-atom binding sites in the interior and surface of the two independent molecules show small but significant deviations from the transformation relating the two molecules; the surface sites show somewhat larger differences than those in the interior of the protein. The packing environs of the two independent molecules show some differences from the environs of the molecules in the tetragonal and triclinic forms, especially in the *C*-terminal region. Also, there is some suggestion of local conformational differences between the two molecules.

Introduction

Hen egg white lysozyme crystallizes in several different polymorphic forms (Steinrauf, 1959), many of which are suitable for X-ray crystallographic study. The structure of the tetragonal form has been determined at 2 Å resolution (Blake, Mair, North, Phillips & Sarma, 1967). The triclinic form has been studied by two different groups: at 2·5 Å resolution by Moult *et al.* (1976) and at 1·5 Å resolution by Hodsdon, Sieker & Jensen (1974). We started work on the monoclinic crystal form containing two independent molecules in the asymmetric unit in 1970. During the course of our studies we found that this form converts into a second monoclinic form (*M*2). Subsequently, we have shown that these two forms can be grown at low (*M*1) and high (*M*2) pH's respectively. Both forms produce high-resolution diffraction data. In this paper we report the structure of the *M*1 form at 4 Å resolution and our ultimate aim is to extend the structure analysis to atomic resolution in order to compare the conformations of the two independent molecules among themselves and with those of the tetragonal and triclinic forms when they are refined. Such a comparative study of the structure of the same protein in a number of different crystal lattices is important to investigate the effects of crystal packing forces on the molecular conformations.

Experimental

Crystallization and the M1 and M2 forms

Crystals were grown in these laboratories by Abola (1970) by a slight modification of the published procedure (Crick, 1953; Steinrauf, 1959). Two distinct monoclinic crystal forms denoted by *M*1 and *M*2 were found; both belong to the space group $P2_1$, contain two molecules of lysozyme in the asymmetric unit, are morphologically indistinguishable and have nearly

* Present address: Department of Chemistry, Harvard University, Cambridge, Massachusetts, USA.

† Present address: Department of Physics and Crystallography, University of Madras, Madras, India.

‡ Present address: Wellcome Research Laboratories, Langley Court, Beckenham, Kent BR3 3BS, England.

§ Present address: Department of Chemistry, Brookhaven National Laboratory, Upton, New York, USA.

‖ To whom all correspondence should be addressed.

0567-7408/81/030591-07$01.00

identical unit-cell parameters ($M1$: $a = 28{\cdot}0$, $b = 62{\cdot}9$, $c = 60{\cdot}5$ Å, $\beta = 90{\cdot}8°$; $M2$: $a = 27{\cdot}5$, $b = 63{\cdot}5$, $c = 60{\cdot}3$ Å, $\beta = 90{\cdot}5°$). Both forms have been produced in a single batch in our early crystallization experiments without buffers. The low-resolution diffraction patterns of both forms show pseudo B-centering (Fig. 1); reflections of the type hkl are systematically weak when $h + l$ is odd. The pseudosymmetry is stronger in the $M2$ form than in the $M1$ form. The r.m.s. difference in the structure amplitudes of $M1$ and $M2$ forms at 6 Å resolution is 45%. Since we have once observed the conversion of the $M1$ form into the $M2$ form, the transition between the two forms may involve a minor reorientation in the crystal. We have since found it possible to control the production of the two forms by adjusting the pH of the crystallization experiment. Indeed, titration experiments indicate that the $M2$ form is produced exclusively at pH 7·0 and above while the $M1$ form is produced exclusively at pH 6·8 and below. Such a sharp transition indicates that it may be related to the ionization of one or more amino acid residues. Interestingly, the only residue which ionizes near pH 6·9 is Glu 35 (Imoto, Johnson, North, Phillips & Rupley, 1972).

In this paper, the structural studies of the low-pH form are reported. The conditions used for obtaining crystals of the $M1$ form were: a 1% (w/v) solution of hen egg white lysozyme (Worthington Biochemical Co.) in 0·05 M sodium aspartate buffer (pH 4·4) was filtered through a 0·22 μm 'Millex' millipore filter and brought to 2·5% in sodium nitrate. The solution was allowed to stand undisturbed in the dark at room temperature and crystal growth was generally complete in two to three days. Crystals grown by this technique develop as large monoclinic plates with crystals as large as 2·0 × 1·0 × 0·6 mm being common. The crystals diffract strongly to about 1·5 Å resolution and are highly stable to X-irradiation.

Preparation of heavy-atom derivatives

About two dozen compounds were investigated for potential heavy-atom derivatives by soaking pregrown native crystals in solutions containing appropriate heavy-atom reagents. Some of the heavy-atom reagents resulted in the interconversion of the crystal forms which complicated the initial studies on the search for heavy-atom derivatives. Four heavy-atom derivatives were ultimately identified; *viz* mercuric *p*-chlorobenzenesulfonate (two derivatives differing in degree of substitution, denoted as PCMBS I and II), mercuric nitrate [$Hg(NO_3)_2$] and uranyl nitrate [$UO_2(NO_3)_2$]. The unit-cell constants for these derivatives were within 0·3% of those of the native crystal.

Data collection, data reduction and scaling

The data were collected on an automated Picker FACS-I diffractometer under the control of the Vanderbilt program system (Lenhert, 1975). The crystals were mounted in 1·0 mm glass capillaries with the b axis parallel to the capillary axis. The PCMBS II

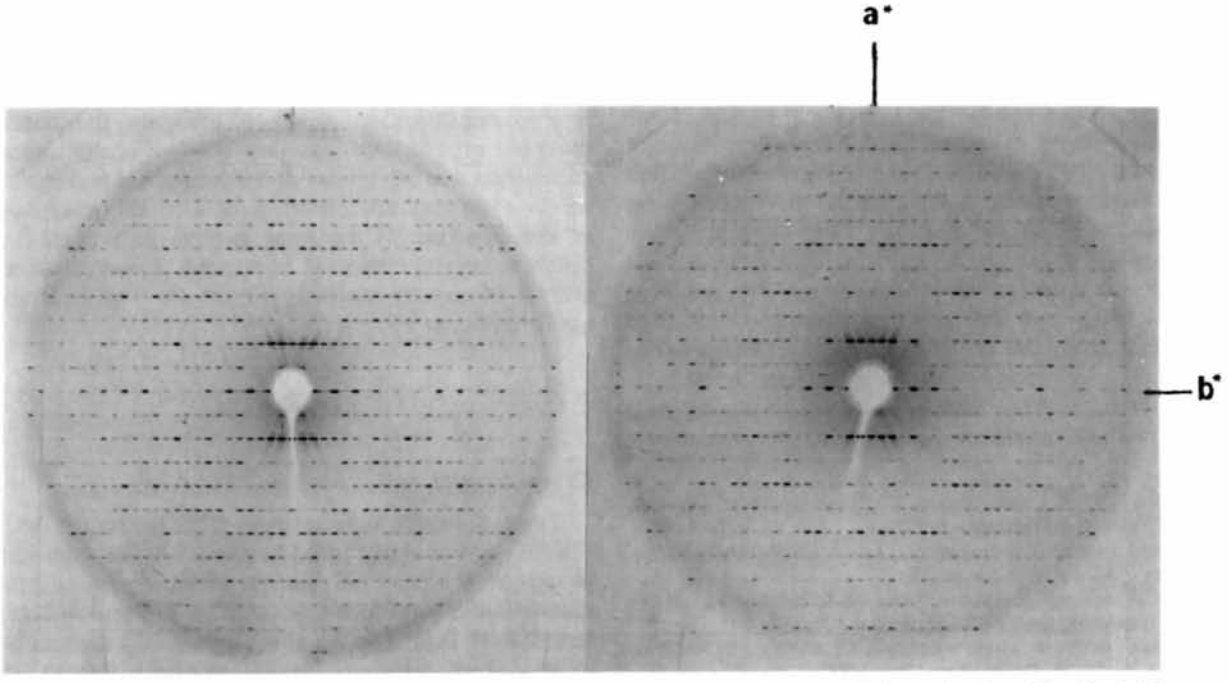

Fig. 1. $hk0$ diffraction patterns of the $M1$ form (left) and the $M2$ form (right). The resolution at the edge of the film is 3 Å.

Table 1. *Data-collection parameters*

Data set	Radiation	Mode	Number of steps	Scan range/step width	Step time	Back-ground	Back-ground time	Reso-lution	Bijvoet pair	Number of reflections
Native	Ni-filtered	$\omega/2\theta$ step	5	0·08°	4 s	0·7°	4 s	3 Å	Yes	9371
PCMBS I	Ni-filtered	$\omega/2\theta$ continuous	–	1·2	–	0·6	10	6	Yes	2286
PCMBS II	Monochromatized	$\omega/2\theta$ step	5	0·085	4	0·7	4	3·8	Yes	4200
$Hg(NO_3)_2$	Ni-filtered	$\omega/2\theta$ step	7	0·09	4	0·75	4	4	Yes	3891
$UO_2(NO_3)_2$	Ni-filtered	$\omega/2\theta$ step	7	0·10	4	0·80	4	6	No	578

data were collected using Cu $K\alpha$ radiation and a graphite monochromator. All the other data sets were collected with Ni-filtered Cu $K\alpha$ radiation. The data were collected either with an $\omega/2\theta$ continuous scan (PCMBS I) or with an $\omega/2\theta$ step scan with five steps near the center of the peak (native, PCMBS II, mercuric nitrate and uranyl nitrate). As a rule, Bijvoet pairs were collected at the -2θ position in groups of 30 reflections. A differential absorption correction curve (φ curve) was obtained for each crystal by measuring the intensity of the 0,16,0 reflection at 10° intervals on φ. The parameters relevant to these data sets are listed in Table 1.

The integrated intensities of the data collected by the $\omega/2\theta$ step scan technique were estimated by fitting the observed steps to a Gaussian curve (Watenpaugh, Sieker, Jensen, Legall & Dubourdieu, 1972) of the form: $y_i = C_1 \exp[-C_3(x_i - C_2)^2]$, where C_1 is the peak height, C_2 the peak position and C_3 the half-width of the Gaussian curve and y_i and x_i are the count and position on 2θ for the ith step respectively. The parameters C_1 and C_2 were refined for each reflection, while the parameter C_3 was determined by a least-squares fit of an anisotropic shape function to the peak profiles of the strongest 30% of the reflections in the data set. The intensities of each data set were corrected for background, differential absorption (North, Phillips & Mathews, 1968), Lorentz–polarization effects and crystal decay and converted to structure factor amplitudes. The equivalent reflections within each data set were averaged. The Bijvoet pairs in the PCMBS I, PCMBS II and the mercuric nitrate data sets were kept separate. Derivative data sets were then scaled to the native data using a scale and isotropic thermal parameter.

Phase calculation

Major heavy-atom sites were located for each derivative from three-dimensional isomorphous difference Patterson syntheses. In PCMBS I, PCMBS II and mercuric nitrate derivatives, anomalous and combination difference Patterson maps (Kartha & Parthasarathy, 1965; Matthews, 1966) were also calculated and these were consistent with the isomorphous difference Patterson maps.

Table 2. *Refined heavy-atom parameters*

The estimated standard deviations are ~1–3 e in occupancies and 0·05–0·20 Å in the positions.

Site	Occupancy (e)	x	y	z	B (Å²)	r.m.s. difference from native F
$Hg(NO_3)_2$						0·16
Hg1	83·63	0·4057	0·1650	0·6703	15	
Hg2	24·36	0·8172	0·1597	0·2210	15	
Hg3	31·63	0·1194	0·4894	0·4126	15	
Hg4	14·11	0·9330	0·2427	0·1806	15	
PCMBS II						0·16
PCMBS1	64·00	0·2907	0·4900	0·4089	16	
PCMBS2	81·21	0·4792	0·1422	0·6810	15	
PCMBS3	47·60	0·7799	0·4510	0·9123	14	
PCMBS4	26·61	0·8413	0·1627	0·2281	15	
PCMBS5	15·90	0·6300	0·1832	0·9671	15	
PCMBS6	22·35	0·1530	0·3376	0·6470	15	
PCMBS7	26·12	0·1323	0·4467	0·7455	15	
PCMBS I						0·16
PCM1	70·00	0·2739	0·4900	0·4081	15	
PCM2	79·74	0·4779	0·1424	0·6879	15	
PCM3	40·51	0·7881	0·4597	0·9084	15	
PCM4	29·47	0·8057	0·1732	0·2132	15	
$UO_2(NO_3)_2$						0·19
U1	77·46	0·4392	0·1441	0·7264	15	
U2	77·00	0·8158	0·1500	0·2605	15	

The positions, occupancies and thermal parameters of the heavy-atom sites in the PCMBS I, PCMBS II and mercuric nitrate derivatives were refined by using the combination coefficients. The sites in different derivatives were correlated in the usual way. The hand of the derivatives was established with a Bijvoet difference Fourier map calculated for the PCMBS I derivative (Kraut, 1968). The final cycles of heavy-atom refinement and phase calculation were carried out by the standard technique (Blow & Crick, 1959) using four derivatives where the occupancies and thermal parameters of the sites were adjusted in alternate cycles. The data from the PCMBS I and uranyl derivatives were limited to 6 Å resolution. During the refinement, three additional minor sites in the PCMBS II derivative were detected in difference Fourier maps. After the final cycle of refinement, 1664 reflections with $F > 6\sigma(F)$ in the range $4 < d < 15$ Å were phased with

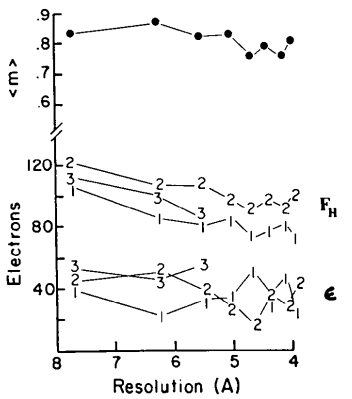

Fig. 2. The variation of the r.m.s. lack of closure ε, the r.m.s. heavy-atom contribution F_H and the mean figure of merit $\langle m \rangle$ with resolution. The numbers in the plot refer to the derivatives: (1) $Hg(NO_3)_2$, (2) PCMBS and (3) $UO_2(NO_3)_2$.

a mean figure of merit of 0·80. The heavy-atom parameters are listed in Table 2 and the refinement statistics shown in Fig. 2.

Results

The 'best' phases were used to calculate a native electron density map which was sectioned on the x axis on a 0·8 × 0·9 × 0·9 Å grid, plotted on a scale of 0·5 "/Å (1·3 cm/Å), contoured in equal but arbitrary intervals, transferred to glass sheets and studied in a light box. Despite several areas of close contacts between molecules, the molecular boundaries were readily apparent in the map. Closer inspection of the map clearly revealed three stretches of right-handed α helix and a single turn of antiparallel β sheet in each molecule. The backbone was traced by placing small gummed labels separated by about 1·5 Å in the densities. These labels do not necessarily correspond to α-carbon atoms. The tracing was straightforward except for the regions of residues 40–50 (β strand) and 64–76 (hairpin loops) in both molecules where weak densities and close contacts with neighboring molecules made the chain tracing somewhat ambiguous. In such regions, the tetragonal model (Blake *et al.*, 1967; Imoto *et al.*, 1972) was used in establishing chain connectivity.

A preliminary model of each of the two independent lysozyme molecules was derived by measuring the coordinates of the gummed labels ('pseudo atoms') used to trace the polypeptide backbone of each molecule and obtaining the transformations (Rao & Rossmann, 1973) to relate them to the α-carbon coordinates of the tetragonal crystal form (Imoto *et al.*, 1972). For molecule A, 92 of the 129 α-carbon atoms of the tetragonal model were fitted to the corresponding pseudo atoms with an r.m.s. deviation of 1·34 Å, while for molecule B, 90 of the 129 α-carbon atoms were fitted with an r.m.s. deviation of 1·07 Å. The rotation matrices and translation vectors for the two molecules are given in Table 3. Fig. 3 shows the backbone chain trace for molecules A and B and the α-carbon backbone of the tetragonal model in a similar orientation.

Table 3. *Transformations for positioning the tetragonal lysozyme structure in the monoclinic unit cell*

X monoclinic = [**R**] **X** tetragonal + **T**.

The tetragonal coordinates and the monoclinic coordinates refer to orthogonal ångström systems. The orthogonal monoclinic system is a,b,c^*.

Molecule *A*			
	0·83439	0·45161	−0·31597
R =	−0·19522	−0·29396	−0·93567
	−0·51544	0·84240	−0·15711
T =	−3·7976	57·0700	9·6321
Molecule *B*			
	−0·81849	−0·29248	0·49450
R =	−0·42247	−0·27691	−0·86304
	0·38936	−0·91530	0·10308
T =	−17·8835	84·9293	−36·6348

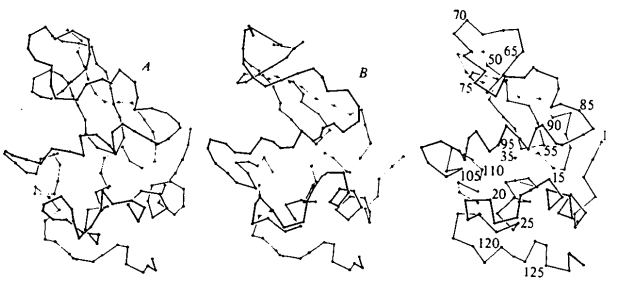

Fig. 3. Backbone trace for molecule A (left) and molecule B (middle). The circles represent a subset of points found in the actual backbone tracing in the 4 Å MIR map. An α-carbon diagram of the tetragonal model is shown at the right in a similar orientation for comparison.

The atomic coordinates derived by the application of these transformations to the complete set of atomic coordinates of the tetragonal lysozyme produced an R value ($R = \sum |F_o - F_c| / \sum F_o$) of 0·43 for the 1701 reflections with $4 < d < 15$ Å and $F_o > 3\sigma(F_o)$.

Discussion

Pseudosymmetry and heavy-atom binding sites

The two independent molecules are related approximately by a translation of $a/2$, 0, $c/2$. The rotation matrix and translation vector that relates the Cartesian coordinates of the two molecules $\mathbf{X}_A$ and $\mathbf{X}_B$ are:

$$\mathbf{X}_A = \begin{bmatrix} 0{\cdot}971 & 0{\cdot}205 & 0{\cdot}121 \\ 0{\cdot}217 & 0{\cdot}971 & -0{\cdot}097 \\ -0{\cdot}098 & 0{\cdot}120 & 0{\cdot}988 \end{bmatrix} \mathbf{X}_B + \begin{bmatrix} -14{\cdot}65 \\ 4{\cdot}78 \\ -31{\cdot}23 \end{bmatrix}.$$

The deviations from exact *B*-centering imply that the two independent molecules have slightly different crystalline environments as seen by the small differences in the packing contacts of the two molecules (see below) and in the binding of heavy atoms to the two independent molecules.

The compounds used to prepare the heavy-atom derivatives in this study are known to differ in the nature of their binding to proteins (Blundell & Jenkins, 1977). Despite these differences, the heavy-atom binding sites for all three derivatives are very similar and may be divided into two classes. The first class of sites is located in the pocket formed by the bend between the helices 80–85 and 90–100 and the helix 5–15 of one molecule and the hairpin loop region 69–74 of a pseudosymmetry-related molecule (Fig. 3). The heavy-atom sites which belong to this class are: Hg1, PCMBS2 and U1 (in which the pocket is between the helices in molecule *A*) and Hg2, PCMBS4 and U2 (in which the pocket is between the helices in molecule *B*). The second class of sites is located deep within the active cleft of the lysozyme molecule (Fig. 4). The heavy atoms which belong to this class are PCMBS1 and Hg3 (binding in the active site of molecule *B*).

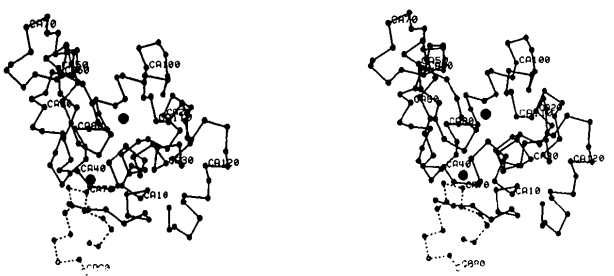

Fig. 4. A stereofigure showing the two classes (see text) of heavy-atom binding sites in monoclinic lysozyme represented here by α-carbon atoms.

Table 4. *Differences in heavy-atom sites in molecules A and B*

Pair of sites	Difference in position*	Difference in occupancy
Hg1–Hg2	3·6 Å	60 e
PCMBS2–PCMBS4	4·4	54
U1–U2	3·6	0
PCMBS1–PCMBS3	1·1	16

* The positional differences in the heavy-atom sites were measured by transforming molecule *B* into molecule *A* using the transformation shown in the text.

The binding of metal ions generally conforms to the pseudosymmetry in the crystal. In the PCMBS derivative, sites 1 and 3 and sites 2 and 4 are paired and in the mercury derivatives, sites 1 and 2 are paired. However, the pairing is not exact; there are significant differences in both the positions and occupancies of 'equivalent' sites in the two molecules (Table 4). The differences in the positions of paired sites are particularly large for PCMBS2–PCMBS4, Hg1–Hg2 and U1–U2 which are at the molecular surface and would be expected to be very sensitive to the relative orientation of the molecules which form the intermolecular interface. The positional differences are much smaller for the PCMBS1–PCMBS3 sites which are located in the active-site cleft and involve ligands from one molecule only. However, there is a significant difference in the occupany of the sites in molecules *A* and *B* suggesting that even within the active-site cleft there are some differences in local environment and/or conformation in the two molecules.

Molecular packing in the monoclinic, tetragonal and triclinic crystals

The packing of the α-carbon models of the two lysozyme molecules in the monoclinic cell is shown in Fig. 5. The volume occupied per dalton of the protein is 1·83 Å^3 for monoclinic lysozyme, 1·81 Å^3 for triclinic and 2·04 Å^3 for tetragonal forms compared with the average value of 2·4 Å^3 for proteins (Matthews, 1969). Thus, the monoclinic and triclinic forms are very tightly packed. Despite the tight packing and the fact that our model was derived by molecular replacement of the tetragonal model into the monoclinic cell, there are only 14 intermolecular contacts less than 6 Å between the α-carbon atoms (Table 5). Seven of the close contacts involve α-carbon atoms within three residues of the amino or the carboxy terminus of one of the molecules and can be easily relieved by a small adjustment of the free ends of the molecule. The remaining contacts may indicate regions of the molecule where small but significant main-chain conformational differences exist between the two crystal forms. In addition, there are some close contacts between the atoms of the side

Table 5. *Intermolecular* Cα–Cα *contacts* ≤ 6 Å

Residues	Symmetry code*	Distance (Å)	Residues	Symmetry code*	Distance (Å)
*A*1–*B*′47	2, 1 0 1	4·94	*A*82–*B*′117	1, −1 0 −1	5·06
*A*1–*B*′48	2, 1 0 1	5·14	*A*82–*B*′118	1, −1 0 −1	3·96
*A*2–*B*′49	2, 1 0 1	4·91	*A*117–*B*′90	1, 0 0 0	5·34
*A*22–*B*′81	1, −1 0 0	5·46	*B*107–*B*′126	2, 1 −1 2	4·26
*A*47–*A*′77	1, 1 0 0	5·80	*B*107–*B*′127	2, 1 −1 2	4·90
*A*78–*B*′117	1, −1 0 −1	5·56	*B*107–*B*′128	2, 1 −1 2	5·17
*A*79–*B*′113	1, −1 0 −1	5·71	*B*109–*B*′128	2, 1 −1 2	5·15

* Symmetry element, and unit translation on *x*,*y*,*z* which generates the coordinates of molecule *B*′ from molecule *B*. Symmetry element (1) *x*,*y*,*z*; symmetry element (2) $\bar{x}, \frac{1}{2} + y, \bar{z}$.

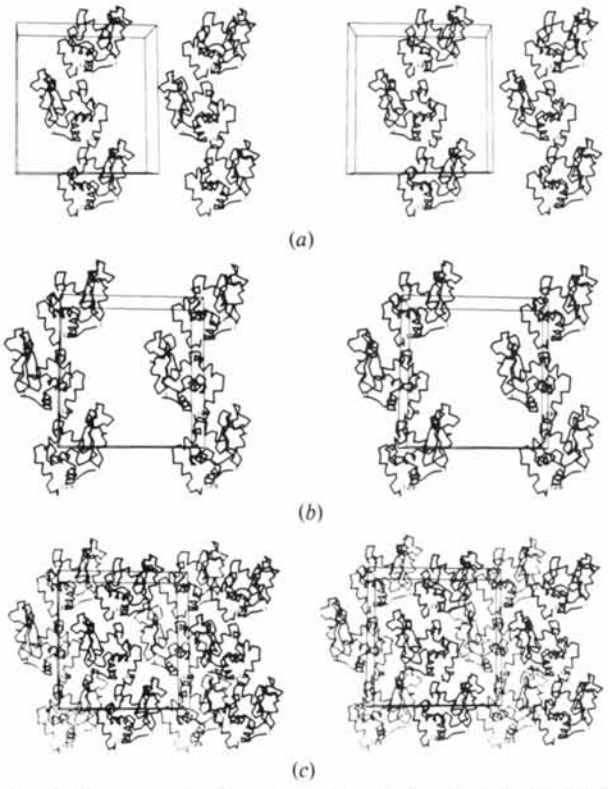

Fig. 5. Stereo packing diagrams of the α-carbon atom model of the two independent molecules of the monoclinic lysozyme (*M*1) viewed down the *a* axis. (*a*) Molecule *A* only, (*b*) molecule *B* only, and (*c*) both molecules *A* (solid) and *B* (dashed).

chain and backbone which will require these side chains to assume different conformations. The most significant of these involves Trp 62 in both molecules which is also implicated in substrate binding in the tetragonal form (Imoto *et al.*, 1972).

The intermolecular interfaces which characterize the crystal packing include interactions between molecules related by the pseudosymmetry and crystallographic symmetry. The principal interactions between pseudosymmetry-related molecules are: (*a*) between the short helical segment 79–84 of one molecule and the bend between the two short helical segments 108–115 and 119–122 of a translation($\sim a/2$, 0, $\sim c/2$)-related molecule and (*b*) the *N*-terminal segment 1–5 of one molecule approaching the segments 46–50 and 69–72 (both tight bends) of a non-crystallographic screw-related molecule. Interactions between molecules related by crystallographic symmetry are: (*a*) approach of the *C*-terminal segment 125–129 and the top (*N*-terminal) of the helix 5–15 of one molecule into the mouth of the active-site cleft (residues 62–64 and 101–109) of a screw-related molecule and (*b*) approach of residues 34–37 and 45–46 of one molecule to residues 14–16 and 75–79 respectively of a molecule related by a unit-cell translation along the *a* axis.

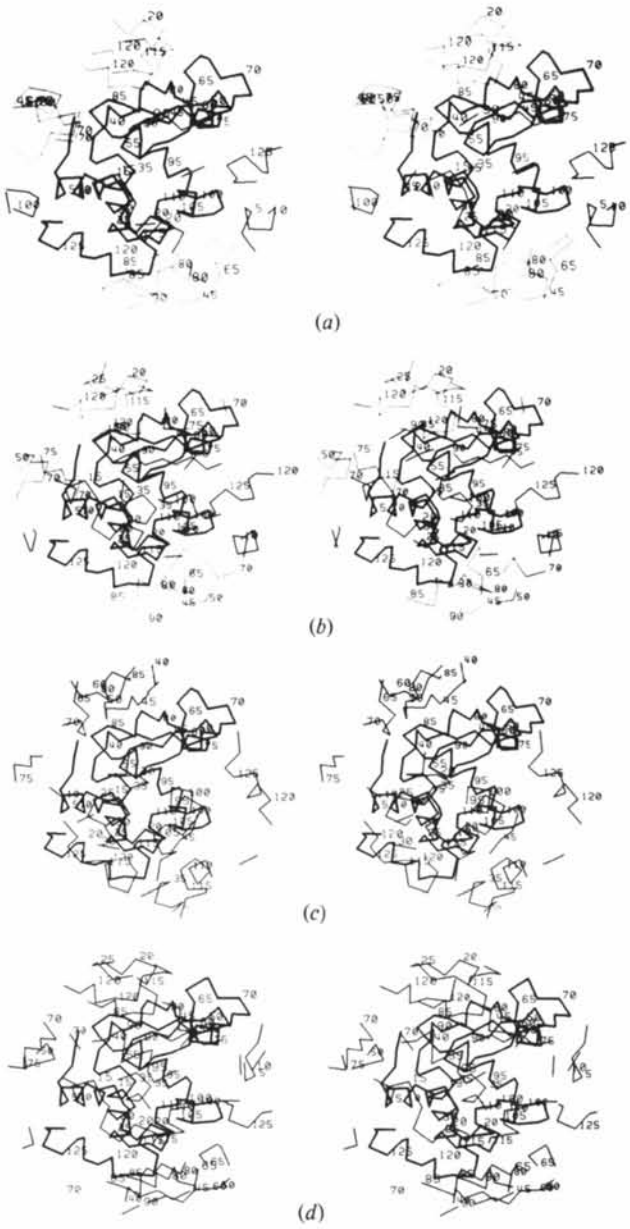

Fig. 6. The lysozyme molecule is shown in similar orientations in these figures. In addition, α-carbon atoms within a sphere of radius 25 Å from the molecular center belonging to symmetry-related molecules are also shown. (*a*) Monoclinic, molecule *A*, (*b*) monoclinic, molecule *B*, (*c*) tetragonal, and (*d*) triclinic.

The intrusion of the *C*-terminus into the active-site cleft results in the partial occlusion of the lower region of the active site in the monoclinic crystals and the approach of residues His 15 and Glu 35 may be of special interest in the light of the proposed interaction of these residues on the pH-dependent self-association of lysozyme in solution (Shindo, Cohen & Rupley, 1977).

Identical views of the lysozyme molecules (*A* and *B* of the monoclinic form and tetragonal triclinic forms) are shown in Fig. 6 with parts of symmetry-related molecules within 25 Å of the molecular center. In spite of the different crystal symmetries, there is a remarkable similarity in the intermolecular contacts, with the incursion of the *C*-terminal region into the active-site cleft being the common motif. It is significant that, in spite of the general similarities of the molecular environment in different crystal forms, suggestions of conformational changes between them and the two molecules in the monoclinic form are evident even in the 4 Å MIR map. We plan to carry out a high-resolution study of the monoclinic form for a comparison of the conformations of the two molecules with those of the tetragonal and triclinic forms. It is envisaged that such an investigation would provide some interesting insights into the conformational fluctuations of proteins.

We gratefully acknowledge support of this research by NSF grant PCM76-23288 and NIH grant GM-18455 and the College of Agricultural and Life Sciences, University of Wisconsin–Madison.

References

ABOLA, J. (1970). Unpublished results.

BLAKE, C. C. F., MAIR, G. A., NORTH, A. C. T., PHILLIPS, D. C. & SARMA, V. R. (1967). *Proc. R. Soc. London Ser. B*, **167**, 365–377.

BLOW, D. M. & CRICK, F. H. C. (1959). *Acta Cryst.* **12**, 794–802.

BLUNDELL, T. L. & JENKINS, J. A. (1977). *Chem. Soc. Rev.* **6**, 139–181.

CRICK, F. H. C. (1953). *Acta Cryst.* **6**, 221–222.

HODSDON, J. M., SIEKER, L. C. & JENSEN, L. H. (1974). Am. Crystallogr. Assoc. Spring Meeting. Abstract J8.

IMOTO, T., JOHNSON, L. N., NORTH, A. C. T., PHILLIPS, D. C. & RUPLEY, J. A. (1972). *The Enzymes*, 3rd ed., edited by P. D. BOYER, pp. 665–868. New York: Academic Press.

KARTHA, G. & PARTHASARATHY, R. (1965). *Acta Cryst.* **18**, 745–749.

KRAUT, J. (1968). *J. Mol. Biol.* **35**, 511–512.

LENHERT, P. G. (1975). *J. Appl. Cryst.* **8**, 568–570.

MATTHEWS, B. W. (1966). *Acta Cryst.* **20**, 82–86.

MATTHEWS, B. W. (1969). *J. Mol. Biol.* **33**, 491–497.

MOULT, J., YONATH, A., TRAUB, W., SMILANSKY, A., PODJORNY, D., RABINOVICH, D. & SAYA, A. (1976). *J. Mol. Biol.* **100**, 179–195.

NORTH, A. C. T., PHILLIPS, D. C. & MATHEWS, F. S. (1968). *Acta Cryst.* A**24**, 351–359.

RAO, S. T. & ROSSMANN, M. G. (1973). *J. Mol. Biol.* **76**, 241–256.

SHINDO, H., COHEN, J. S. & RUPLEY, J. A. (1977). *Biochemistry*, **16**, 3879–3882.

STEINRAUF, L. K. (1959). *Acta Cryst.* **12**, 77–79.

WATENPAUGH, K. D., SIEKER, L. C., JENSEN, L. H., LEGALL, L. & DUBOURDIEU, M. (1972). *Proc. Natl Acad. Sci. USA*, **69**, 3185–3188.

Acta Cryst. (1981). B**37**, 597–601

Internal Water Bridge and Antiparallel Sheet in the Structure of Benzyloxycarbonyl-L-alanyl-D-phenylalanyl-L-proline Monohydrate

BY C. M. K. NAIR, R. NAGARAJ, S. RAMAPRASAD, P. BALARAM AND M. VIJAYAN

Molecular Biophysics Unit, Indian Institute of Science, Bangalore 560012, *India*

(*Received* 7 *August* 1980; *accepted* 25 *September* 1980)

Abstract

Benzyloxycarbonyl-L-alanyl-D-phenylalanyl-L-proline monohydrate, $C_{25}H_{29}N_3O_6.H_2O$, crystallizes in the orthorhombic space group $P2_12_12_1$ with four molecules in a unit cell of dimensions $a = 9{\cdot}594$ (9), $b = 9{\cdot}705$ (4) and $c = 27{\cdot}917$ (12) Å. The structure has been refined to an R value of 0·067 for 2046 observed reflections. All the peptide units in the molecule are *trans* and the prolyl residue is in the C_2–C^{γ}-*exo*–C^{β}-*endo* conformation. The lone water molecule in the structure is hydrogen bonded to the carbonyl O atom in the benzyloxycarbonyl group and to one of the O atoms in the terminal carboxyl group. This internal water bridge, observed for the first time in a linear peptide, provides a model for water-mediated chain-reversal. An interesting feature of the crystal structure is the presence of an antiparallel sheet involving the alanyl and the phenylalanyl residues.

Introduction

Structural studies on small proline-containing peptides with all L, and mixed L and D sequences are valuable in

0567-7408/81/030597-05$01.00